

## Anomalous Auger Recombination in PbSe

Xie Zhang<sup>1,\*</sup>, Jimmy-Xuan Shen,<sup>2</sup> and Chris G. Van de Walle<sup>1,†</sup>

<sup>1</sup>*Materials Department, University of California, Santa Barbara, California 93106-5050, USA*

<sup>2</sup>*Department of Physics, University of California, Santa Barbara, California 93106-9530, USA*



(Received 23 December 2019; accepted 29 June 2020; published 13 July 2020)

Using first-principles approaches we find that the Auger recombination in PbSe is anomalous in three distinct ways. First, the direct Auger coefficient is 4 orders of magnitude lower than that of other semiconductors with similar band gaps, a result that can be attributed to the lack of involvement of a heavy-hole band. Second, phonon-assisted indirect Auger recombination prevails, contrary to the common belief that direct Auger is dominant in narrow-gap semiconductors. Third, an unexpectedly weak temperature dependence of the Auger coefficient is observed, which we can now attribute to the indirect nature of the Auger process. The widely accepted explanation of this behavior in terms of an unusual temperature dependence of the band gap is only a secondary effect. Our results elucidate the mechanisms underlying the anomalous Auger recombination in IV-VI semiconductors in general, which is critical for understanding and engineering carrier transport.

DOI: [10.1103/PhysRevLett.125.037401](https://doi.org/10.1103/PhysRevLett.125.037401)

When an excited electron recombines with a hole across the band gap of a semiconductor, the excess energy and momentum can be captured by a third charge carrier, which gets promoted to a higher-lying energy state. If this process involves only the Coulomb interaction between the carriers, it is called *direct* Auger recombination. If additional momentum is provided by scattering (for instance from phonons), the Auger process is labeled *indirect*.

As a third-order process, Auger recombination affects the microscopic carrier dynamics at high carrier densities, thus impacting the operation of many semiconductor devices. In particular, Auger has been shown to govern the performance of infrared detectors [1], to be responsible for the efficiency droop of light-emitting diodes [2], and to significantly impact the transport properties of topological insulators [3]. Identifying which Auger process is dominant in specific materials is thus crucial [4–8]. Based on a compilation of literature data, Bulashevich and Karpov [9] observed distinct trends in the Auger coefficient as a function of band gap. For small band gaps ( $\leq 1.0$  eV), the coefficient decreases exponentially with increasing gap. This has conventionally been attributed to the fact that the direct Auger process dominates, with the exponential dependence resulting from the Fermi–Dirac distribution of carriers [10]. For wider-band-gap semiconductors, the Auger coefficient is almost independent of band gap, with a value around  $10^{-31}$ – $10^{-30}$  cm<sup>6</sup> s<sup>-1</sup>. In Ref. [9], this was attributed to the indirect nature of the band gap, in spite of GaN (which has a direct gap) exhibiting the same behavior. It was subsequently shown [2,11,12] that indirect Auger processes, for instance assisted by electron-phonon scattering, can explain these rates, which far exceed those of the direct process in these wider-gap materials.

The narrow-gap semiconductor PbSe (band gap 0.27 eV [13] at room temperature) presents an interesting puzzle: it exhibits a much lower Auger coefficient than would be estimated from the Bulashevich and Karpov plot [9]. In addition, the Auger coefficient has an anomalously weak temperature dependence [14]. In this Letter, we explain both of these features, in the process elucidating the underlying physics. Based on accurate first-principles calculations, we actually find that the *direct Auger coefficient* is 4 orders of magnitude smaller than expected for materials with similar band gaps, and we can correlate this suppression with the lack of involvement of a heavy-hole band. Unexpectedly for such a low-gap material, we find that phonon-assisted *indirect* Auger recombination actually dominates in PbSe. This finding, in turn, explains the weak temperature dependence: the scattering processes in indirect Auger predominantly involve phonon *emission*, which can occur at any temperature. These insights shed new light on the origin of the high efficiency of PbSe as an infrared detector and may offer pathways for overcoming bottlenecks in the efficiency of devices.

To quantitatively compute the Auger coefficient, an accurate characterization of the electronic structure is critical. The computation of the Auger coefficient requires first-principles calculations of eigenvalues, wave functions, and electron-phonon-coupling matrix elements on very dense **k**-point and **q**-point (phonon wave vector) grids. To render this computationally feasible, we use density functional theory (DFT) with the Strongly Constrained and Appropriately Normed (SCAN) functional [15], which has been demonstrated to give a reliable description of the electronic structure of many materials. We benchmark the accuracy of the SCAN functional against the hybrid

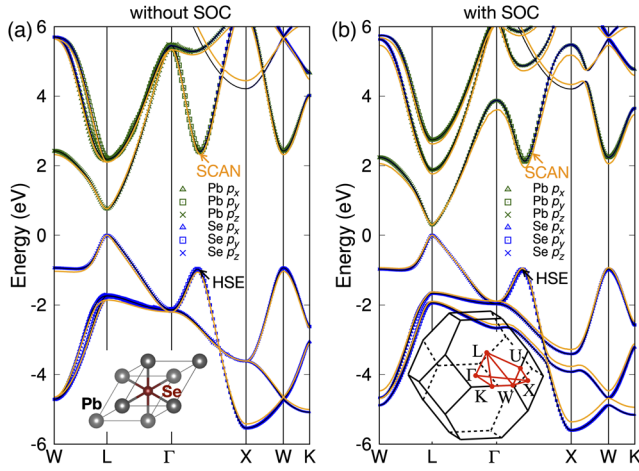


FIG. 1. Comparison of the band structure of PbSe calculated using the SCAN and HSE functionals (a) without SOC and (b) with SOC. The green and blue symbols show the projected orbital character of the bands for the case with the HSE functional. The energy values are referenced to the VBM. The band gap of the SCAN band structure is scissors-shifted to match the HSE gap. The inset in (a) shows the primitive cell of PbSe, and the inset in (b) depicts the corresponding Brillouin zone and high-symmetry  $k$  points.

functional of Heyd, Scuseria, and Ernzerhof (HSE) [16], as well as experimental results [13]. The details are provided in the Supplemental Material [17].

Figure 1 shows a comparison of the band structures calculated using the SCAN and HSE functionals for rocksalt PbSe [see the inset of Fig. 1(a)]. The two functionals produce quantitatively similar band structures without spin-orbit coupling (SOC) and with SOC. This is true especially in the vicinity of the conduction-band minimum (CBM) and valence-band maximum (VBM), the regions of the band structure that are most likely to participate in the Auger recombination. The calculated effective masses of both electrons and holes are similar between the two functionals and agree very well with experiment [13] (see Supplemental Material [17]). These checks justify the use of the SCAN functional for our Auger calculations in this work.

We start by calculating the direct Auger process (see Supplemental Material [17]), which is commonly accepted to be the dominant mechanism in narrow-gap semiconductors. A scissors shift on the band gap is employed as a proxy for investigating the dependence of the Auger coefficient on band gap. As shown by the insets in Fig. 2, there are two types of direct Auger processes: electron-electron-hole (eeh) vs hole-hole-electron (hhe), depending on the nature of the third carrier (electron vs hole). In Fig. 2, we plot the calculated direct Auger coefficient as a function of the scissors-shifted band gap for both the eeh and hhe processes at room temperature and for a typical carrier density of  $10^{18} \text{ cm}^{-3}$ . We can extract five important insights from these results.

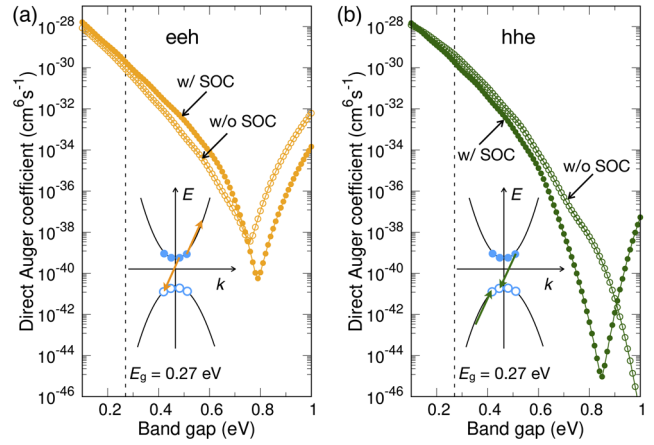


FIG. 2. Calculated direct Auger coefficient (with and without SOC) as a function of band gap for (a) the eeh and (b) the hhe process. A temperature of 300 K and a carrier density of  $10^{18} \text{ cm}^{-3}$  are assumed. The insets schematically show the eeh and hhe direct Auger processes. The light-blue solid (open) circles represent electrons (holes). The black dashed lines indicate the location of the experimental band gap of PbSe at room temperature.

First, for band gaps in the vicinity of the room-temperature experimental gap of 0.27 eV, SOC has only a minor impact on the Auger coefficient. This can be understood based on the orbital characters of the bands (see Fig. 1) and point-group symmetry. The lowest three conduction bands (CBs) comprise Pb  $p$  states, while the highest three valence bands (VBs) consist of Se  $p$  states. The L point has  $D_{3d}$  ( $\bar{3}m$ ) point-group symmetry, which already in the absence of SOC splits off the  $p_z$  state from the degenerate  $p_x$  and  $p_y$  states [22,23]. The Pb  $p_x/p_y$  states occur at  $\sim 1.4$  eV above the CBM, while the Se  $p_x/p_y$  states are at  $\sim 1.7$  eV below the VBM (and comprise the heavy-hole band). The inclusion of SOC further splits the  $p_x$  and  $p_y$  states. These splittings are pronounced, but since these bands are relatively far away from the band edges the splittings only affect the onset of the increase of the Auger coefficient at larger band gaps, as shown in Fig. 2 [24].

Second, this upturn in the Auger coefficients occurs at band gaps around 0.8 eV. It may seem strange to attribute this increase to excitation of carriers to higher bands that occur only at 1.58 eV above the CBM and 1.66 eV below the VBM (at L, in the case with SOC). Previously, we have shown that a resonance of the band gap with the energy separation between the first and second CB (or VB) causes a broad peak in the Auger coefficient as a function of band gap [25,26]. The onset of this broad peak occurs at gaps that are much smaller than the energy separation between the bands for two reasons: i) at a density of  $10^{18} \text{ cm}^{-3}$ , electrons (holes) occupy states with energies more than 0.2 eV from the CBM (VBM); and ii) the energy separation between the first and second CB or VB decreases when moving away from L (Fig. 1).

Third, the inclusion of SOC reduces the equilibrium band gap from 0.76 eV to 0.30 eV in our HSE calculations, but it has only a minor impact on the dependence of the Auger coefficients on band gap in the relevant range near the experimental gap. The differences that occur are due to slight changes in the shape of bands. The direct Auger coefficients are dominated by the magnitude of the band gap.

Fourth, at the experimental room-temperature band gap of 0.27 eV, the calculated Auger coefficients for eeh and hhe processes are almost equal:  $\sim 1.9 \times 10^{-30} \text{ cm}^6 \text{ s}^{-1}$  for eeh and  $\sim 1.8 \times 10^{-30} \text{ cm}^6 \text{ s}^{-1}$  for hhe. This similarity arises because the lowest CB and highest VB are almost mirror images of each other (Fig. 1).

And fifth, these values of Auger coefficients are as much as 4 orders of magnitude smaller than in other semiconductors with similar band gaps, e.g.,  $\text{Hg}_{0.7}\text{Cd}_{0.3}\text{Te}$  [27], and also significantly smaller than experimental values [14,28]. The major reason for the small values is that the highest VB in PbSe is a very dispersive light-hole band, which is almost a mirror image of the lowest CB; the heavy-hole band, at  $\sim 1.7$  eV below the VBM, does not contribute to Auger recombination at energies around the band gap. In contrast, in  $\text{Hg}_{0.7}\text{Cd}_{0.3}\text{Te}$  and most conventional III-V semiconductors the heavy-hole band appears near the gap [29]. The lack of involvement of a heavy-hole band in PbSe makes the simultaneous satisfaction of energy and momentum conservation difficult, resulting in low direct Auger coefficient.

As for experimental values of Auger coefficients, room-temperature values have been reported by two groups, with results differing by an order of magnitude:  $0.8 \times 10^{-27} \text{ cm}^6 \text{ s}^{-1}$  [14] vs  $1.1 \times 10^{-28}$  [28]. A potential concern in comparing with calculations is that the Auger rates may depend on carrier density. In Fig. 3(a) we investigate this dependence. The direct Auger coefficient slightly increases with decreasing carrier density, reaching a plateau below

$10^{17} \text{ cm}^{-3}$ . The carrier density in the experiments of Refs. [14,28] was not reported, but even our highest calculated direct Auger coefficient is more than an order of magnitude smaller than the lower of the experimental values. This discrepancy leads us to question the validity of the assumption that direct Auger is responsible for the experimentally observed rates.

Given the uncertainties in the reported experimental values, it is fruitful to examine *trends*, for instance by calculating the temperature dependence of the Auger coefficient, as shown in Fig. 3(b). If the band gap is fixed at the room-temperature value (0.27 eV), the direct Auger coefficient drops by more than 10 orders of magnitude when the temperature is lowered from 300 to 50 K, in distinct disagreement with experiment, which observes a very weak dependence [14]. What is missing from this description is the fact that the band gap of PbSe decreases with decreasing temperature, and this will enhance the Auger coefficient at low temperatures, as suggested by Findlay *et al.* [14]. We can take the temperature dependence of band gap into account by fitting a fourth-order polynomial to the experimental band gaps at various temperatures [30,31] (see Supplemental Material [17]). After including the temperature dependence of band gap, the decline in the direct Auger coefficient with decreasing temperature is less drastic but still much more pronounced than in experiment, as seen in Fig. 3(b). The decrease in the Auger rate can be attributed to the fact that at low temperatures the carriers occupy a very narrow range of momenta in the vicinity of the L point, making simultaneous conservation of energy and momentum difficult in a direct Auger event.

We are thus confronted with a serious discrepancy between theory and experiment, both for the actual value of the Auger coefficient at room temperature and for the behavior of the Auger rate as a function of temperature. Of course, the comparison implicitly assumed that the direct Auger process dominates the Auger rate—an assumption that has universally been taken for granted in such a low-band-gap material. The observed discrepancy prompts us to reexamine this assumption and explicitly calculate indirect Auger processes.

The calculated phonon-assisted indirect Auger coefficient as a function of carrier density and temperature is shown in Fig. 3 (for details see the Supplemental Material [17]). Unexpectedly, the room-temperature indirect Auger coefficients are an order of magnitude larger than the direct coefficients for a wide range of carrier densities [Fig. 3(a)]. For a density of  $10^{17} \text{ cm}^{-3}$ , the total (eeh + hhe) indirect Auger coefficient is  $\sim 1.1 \times 10^{-28} \text{ cm}^6 \text{ s}^{-1}$  at room temperature, which agrees well with the experimental values [14,28], considering the uncertainties in experiment.

The indirect Auger coefficient also exhibits a relatively weak temperature dependence [Fig. 3(b)]. This is true even if the band gap is fixed at the room-temperature value;

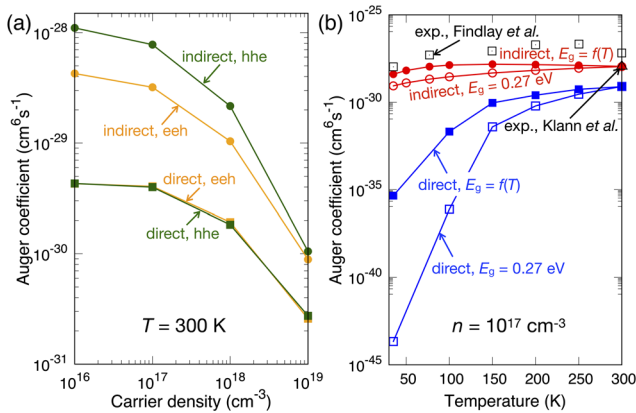


FIG. 3. (a) Calculated Auger coefficients as a function of carrier density at 300 K. (b) Calculated Auger coefficients as a function of temperature at a fixed carrier density of  $10^{17} \text{ cm}^{-3}$ . Experimental data [14,28] are included for comparison.

taking the proper temperature dependence of the gap into account further weakens the temperature dependence, but this is only a secondary effect. We note that weak temperature dependence is a common feature of many other systems where indirect Auger is dominant [32,33]. The reason is that the scattering processes in indirect Auger mainly involve phonon *emission*, which does not require a finite thermal phonon population and can occur at any temperature (see Supplemental Material [17] for a detailed analysis). Phonon *absorption* does depend on the phonon population and leads to a slight increase in Auger rates at higher temperatures.

We thus find that Auger rates in PbSe are dominated by indirect Auger processes. The temperature dependence of indirect Auger is in complete agreement with the weak variation with temperature observed in experiment. We therefore attribute the experimentally measured Auger coefficient of PbSe to phonon-assisted indirect Auger recombination.

We now return to the underlying reasons for the direct Auger coefficient to be anomalously low in PbSe. Previous literature [14,34–36] has also pointed out that the lowest CB and highest VB of PbSe are mirror images of each other and very dispersive. In this situation, low direct Auger coefficients are expected. However, two other factors were commonly cited as counteracting this effect and enhancing the direct Auger coefficient [14,34–36]: i) the presence of degenerate L valleys, and ii) the anisotropy of the band edges. Using our first-principles methodology, we can quantitatively inspect these two factors.

Since the band extrema occur at the L point, a fourfold valley degeneracy is present. Auger recombination can therefore involve intravalley [Fig. 4(a)] as well as intervalley [Fig. 4(b)] events. One may get the impression that intervalley processes can help to enhance the number of momentum-conserved Auger events. However, since for each Auger event the screened Coulomb matrix element contains equal contributions from direct and exchange terms [12], a “direct” intervalley event as shown by the orange arrows in Fig. 4(b) can be equivalently translated to its “exchange” intervalley event [the green dashed arrows in Fig. 4(b)]. Even though this event still occurs across two valleys (L and L’), there is no essential difference between the above intervalley event and an intravalley event since the carriers are equally populated within four L valleys. Hence, the presence of fourfold-degenerate L valleys will not enhance the total Auger coefficient but only distribute the carriers evenly across the valleys.

To inspect the impact of the band anisotropy on momentum conservation, we calculate the momentum transfer (i.e.,  $\Delta\mathbf{k} = \mathbf{k}_1 - \mathbf{k}_2$ ) for all of the momentum-conserved direct Auger events. Figure 4(c) shows the distribution of  $\Delta\mathbf{k}$  in reciprocal space by projecting onto three planes. For all of the momentum-conserved events there is only a slight anisotropy in the momentum transfer,

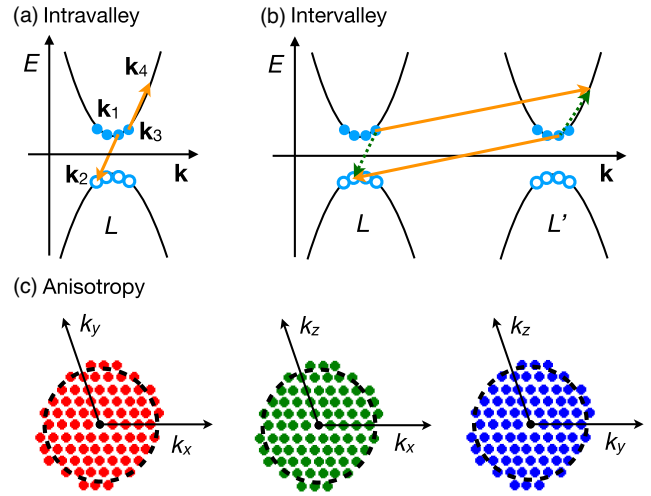


FIG. 4. Schematic of (a) intravalley and (b) intervalley Auger events in PbSe.  $\mathbf{k}_1$  through  $\mathbf{k}_4$  label the momenta of the four states involved in an Auger event. (c) Momentum transfer ( $\Delta\mathbf{k} = \mathbf{k}_1 - \mathbf{k}_2$ ) of all possible Auger events projected onto different planes  $[(k_x, k_y), (k_x, k_z), \text{ and } (k_y, k_z)]$  in reciprocal space. The dashed circles are intended to help visualize the slight anisotropy. We note that since the carrier occupation is evaluated on a discrete  $\mathbf{k}$ -point grid, the momentum transfer is not continuous.

indicating that band anisotropy has only a minor impact on the number of momentum-conserved Auger events.

We conclude that the two commonly invoked factors (degeneracy of the L valleys and anisotropy of the bands) do not significantly enhance the direct Auger coefficient of PbSe; the major reason for the low direct Auger coefficient is the lack of involvement of a heavy-hole band. As for phonon-assisted indirect Auger, since phonons provide additional momentum, the number of momentum-conserved events can be significantly enhanced as compared to direct Auger (see Supplemental Material [17] for more details).

In summary, using first-principles approaches we have systematically investigated the direct and phonon-assisted indirect Auger recombination in PbSe. Contrary to the widely accepted wisdom, we found that direct Auger recombination in this narrow-gap semiconductor is anomalously low and that the Auger rate is actually dominated by the indirect phonon-assisted process. The identified anomalous behavior of the Auger recombination in PbSe is expected to be general for IV-VI semiconductors and calls for a reconsideration of the fundamental mechanisms of Auger recombination in these materials.

We thank Prof. Kunal Mukherjee for fruitful discussions. We acknowledge Prof. Emmanouil Kioupakis for sharing the pseudopotentials of Pb and Se. This work was supported by the U.S. Department of Energy (DOE), Office of Science, Basic Energy Sciences under Award No. DE-SC0010689. Computational resources were provided by

the National Energy Research Scientific Computing Center, a DOE Office of Science User Facility supported by the Office of Science of the DOE under Contract No. DE-AC02-05CH11231.

\*Corresponding author.

xiezhang@ucsb.edu

†Corresponding author.

vandewalle@mrl.ucsb.edu

- [1] M. A. Kinch, *J. Electron. Mater.* **29**, 809 (2000).
- [2] E. Kioupakis, P. Rinke, K. T. Delaney, and C. G. Van de Walle, *Appl. Phys. Lett.* **98**, 161107 (2011).
- [3] Y. Onishi, Z. Ren, K. Segawa, W. Kaszub, M. Lorenc, Y. Ando, and K. Tanaka, *Phys. Rev. B* **91**, 085306 (2015).
- [4] A. Hangleiter and R. Häcker, *Phys. Rev. Lett.* **65**, 215 (1990).
- [5] J. M. Pietryga, K. K. Zhuravlev, M. Whitehead, V. I. Klimov, and R. D. Schaller, *Phys. Rev. Lett.* **101**, 217401 (2008).
- [6] I. Robel, R. Gresback, U. Kortshagen, R. D. Schaller, and V. I. Klimov, *Phys. Rev. Lett.* **102**, 177404 (2009).
- [7] Y. Yamada, H. Yasuda, T. Tayagaki, and Y. Kanemitsu, *Phys. Rev. Lett.* **102**, 247401 (2009).
- [8] J. Iveland, L. Martinelli, J. Peretti, J. S. Speck, and C. Weisbuch, *Phys. Rev. Lett.* **110**, 177406 (2013).
- [9] K. A. Bulashevich and S. Y. Karpov, *Phys. Status Solidi C* **5**, 2066 (2008).
- [10] A. Haug, *J. Phys. C* **16**, 4159 (1983).
- [11] D. Steiauf, E. Kioupakis, and C. G. Van de Walle, *ACS Photonics* **1**, 643 (2014).
- [12] E. Kioupakis, D. Steiauf, P. Rinke, K. T. Delaney, and C. G. Van de Walle, *Phys. Rev. B* **92**, 035207 (2015).
- [13] R. Dalven, *Infrared Phys.* **9**, 141 (1969).
- [14] P. C. Findlay, C. R. Pidgeon, R. Kotitschke, A. Hollingworth, B. N. Murdin, C. J. G. M. Langerak, A. F. G. van der Meer, C. M. Ciesla, J. Oswald, A. Homer, G. Springholz, and G. Bauer, *Phys. Rev. B* **58**, 12908 (1998).
- [15] J. Sun, A. Ruzsinszky, and J. P. Perdew, *Phys. Rev. Lett.* **115**, 036402 (2015).
- [16] J. Heyd, G. E. Scuseria, and M. Ernzerhof, *J. Chem. Phys.* **118**, 8207 (2003).
- [17] See Supplemental Material at <http://link.aps.org/supplemental/10.1103/PhysRevLett.125.037401> for computational details, the polynomial fit of the experimental band gap, the analysis of contribution of different phonons to the indirect Auger coefficients, the analysis of momentum and energy conservation, as well as the contribution of phonon absorption and emission to indirect Auger. The Supplemental Material additionally contains Refs. [18–21].
- [18] P. Giannozzi *et al.*, *J. Phys. Condens. Matter* **21**, 395502 (2009).
- [19] H. J. Monkhorst and J. D. Pack, *Phys. Rev. B* **13**, 5188 (1976).
- [20] P. E. Blöchl, *Phys. Rev. B* **50**, 17953 (1994).
- [21] G. Kresse and J. Furthmüller, *Phys. Rev. B* **54**, 11169 (1996).
- [22] S. Rabii, *Phys. Rev.* **167**, 801 (1968).
- [23] S.-H. Wei and A. Zunger, *Phys. Rev. B* **55**, 13605 (1997).
- [24] Auger coefficients computed for band gaps well above the experimental gap are intended only for discussing trends since the band shape and matrix elements may differ from the ones at the band gap of 0.27 eV.
- [25] J.-X. Shen, X. Zhang, S. Das, E. Kioupakis, and C. G. Van de Walle, *Adv. Energy Mater.* **8**, 1801027 (2018).
- [26] X. Zhang, J.-X. Shen, and C. G. Van de Walle, *Adv. Energy Mater.* **10**, 1902830 (2020).
- [27] A. Rogalski, *Rep. Prog. Phys.* **68**, 2267 (2005).
- [28] R. Klann, T. Höfer, R. Buhleier, T. Elsaesser, and J. W. Tomm, *J. Appl. Phys.* **77**, 277 (1995).
- [29] U. K. Mishra and J. Singh, *Semiconductor Device Physics and Design* (Springer, Netherlands, 2008).
- [30] J. M. Besson, W. Paul, and A. R. Calawa, *Phys. Rev.* **173**, 699 (1968).
- [31] M. Baleva, T. Georgiev, and G. Lashkarev, *J. Phys. Condens. Matter* **2**, 2935 (1990).
- [32] W. Lochmann, *Phys. Status Solidi A* **40**, 285 (1977).
- [33] E. Kioupakis, Q. Yan, D. Steiauf, and C. G. Van de Walle, *New J. Phys.* **15**, 125006 (2013).
- [34] P. R. Emtage, *J. Appl. Phys.* **47**, 2565 (1976).
- [35] O. Ziep, M. Mocker, D. Genzow, and K. H. Herrmann, *Phys. Status Solidi B* **90**, 197 (1978).
- [36] R. Rosman and A. Katzir, *IEEE J. Quantum Electron.* **18**, 814 (1982).